

# International Conference on Space Optics—ICSO 2008

Toulouse, France

14–17 October 2008

*Edited by Josiane Costeraste, Errico Armandillo, and Nikos Karafolas*



## *The Spectropolarimeter for Planetary Exploration: SPEX*

*Erik Laan*

*Daphne Stam*

*Frans Snik*

*Theodora Karalidi*

*et al.*



## THE SPECTROPOLARIMETER FOR PLANETARY EXPLORATION - SPEX

Erik Laan<sup>(1)</sup>, Daphne Stam<sup>(2)</sup>, Frans Snik<sup>(3)</sup>, Theodora Karalidi<sup>(3)</sup>, Christoph Keller<sup>(3)</sup>, Rik ter Horst<sup>(4)</sup>, Ramon Navarro<sup>(4)</sup>, Gijs Oomen<sup>(5)</sup>, Johan de Vries<sup>(5)</sup>, Ruud Hoogeveen<sup>(2)</sup>

<sup>(1)</sup> TNO Science & Industry, P.O. Box 155, 2600 AD, Delft, The Netherlands, E-mail: erik.laan@tno.nl

<sup>(2)</sup> SRON Netherlands Institute for Space Research, Sorbonnelaan 2, 3584 CA Utrecht, the Netherlands, E-mail: d.m.stam@sron.nl

<sup>(3)</sup> Sterrekundig Instituut Utrecht, Princetonplein 5, 3584 CC, Utrecht, the Netherlands, E-mail: f.snik@astro.uu.nl

<sup>(4)</sup> ASTRON Netherlands Foundation for Research in Astronomy, Oude Hoogeveensedijk 4, 7991 PD, Dwingeloo, the Netherlands, E-mail: navarro@astron.nl

<sup>(5)</sup> Dutch Space, Newtonweg 1, 2333 CP Leiden, the Netherlands, E-mail: g.oomen@dutchspace.nl

### ABSTRACT

SPEX (Spectropolarimeter for Planetary EXploration) is an innovative, compact remote-sensing instrument for measuring and characterizing aerosols in the atmosphere. The shoebox size instrument is capable of accurate full linear spectropolarimetry without moving parts or liquid crystals. High precision polarimetry is performed through encoding the degree and angle of linear polarization of the incoming light in a sinusoidal modulation of the spectrum. Measuring this intensity spectrum thus provides the spectral dependence of the degree and angle of linear polarization. Polarimetry has proven to be an excellent tool to study microphysical properties of atmospheric particles. Such information is essential to better understand the weather and climate of a planet. Although SPEX can be used to study any planetary atmosphere, including the Earth's, the current design of SPEX is tailored to study Martian dust and clouds from an orbiting platform. SPEX' 9 entrance pupils can simultaneously measure intensity spectra from 0.4 to 0.8 microns, in different directions along the flight direction (including two limb viewing directions). This way, the scattering phase functions of dust and cloud particles within a ground pixel are sampled while flying over it. SPEX can provide synergy with instruments on rovers and landers, as it provides an overview of spatial and temporal variations of the Martian atmosphere.

### 1. SCIENTIFIC BACKGROUND

Planetary atmospheres contain various types of small particles, so-called aerosol particles. The main aerosol particles in the Martian atmosphere are dust particles that are lifted from the surface due to so-called dust devils, regional storms, or sometimes even global planet-engulfing storms. These global storms develop mostly during the southern Martian spring or summer. Because of the ellipticity of the

Martian orbit around the sun, these are generally warmer than the northern Martian spring and summer. Global storms can develop within 10-15 days and can obscure the Martian surface for weeks to months. At the end of each storm, most of the dust particles settle on the surface. The smallest dust particles, however, remain suspended in the Martian atmosphere and thus form a semi-permanent background dust haze in the Martian atmosphere.

In addition to dust particles, cirrus-like ice clouds have been observed in the Martian atmosphere (see e.g. Pearl et al. 2001). These optically thin clouds consist of water ice particles (at typical altitudes up to about 40 km), or of CO<sub>2</sub> ice particles (at altitudes near about 80 km, where the local temperatures are low enough for CO<sub>2</sub> to freeze).

Accurate knowledge about the spatial and temporal distribution of Martian dust and cloud particles together with their microphysical properties (i.e. their composition, size, and shape) is essential for understanding the many roles these particles play on Mars. They strongly influence the radiative budget and hence a planet's weather and climate system because dust particles scatter and absorb sunlight and thermal radiation from the planet. This is especially true for thin atmosphere of Mars which average surface pressure at "sea"-level is only about 6 mbars, compared to about 1000 mbars on Earth. Additionally, Mars lacks any water bodies that could retain energy, like the oceans do on Earth. Gierasch & Goody (1972) already calculated that the Martian atmospheric temperature could increase up to tens of during large dust storms. Assuming spherical dust particles, Goldenson et al. (2008) show that these temperature changes depend on the size of the dust particles. Because the dust shields the surface from incoming sunlight, the surface temperatures are seen to decrease during storms.

Ice cloud particles also scatter and absorb sunlight and thermal radiation but have a less strong effect

(see e.g. Wilson et al. 2008) on the Martian radiative balance compared to dust particles, because the ice clouds are usually very thin. Nevertheless, water ice clouds are a crucial asset for atmospheric transport of water on Mars (Montmessin et al. 2004). Ice cloud particles also influence the settling of atmospheric dust particles, and hence the cleansing of the atmosphere, since ice cloud particles are thought to usually form on dust particles through heterogeneous nucleation (see e.g. Määttänen et al. 2005),

Besides influencing the Martian radiative balance, dust and ice particles are suspected to enable chemical reactions on their surfaces. This concept is of particular importance concerning the sources and sinks of methane, a gas that might indicate the presence of life on Mars. If, as proposed by e.g. Atreya et al. (2007), methane is removed from the Martian atmosphere during dust storms, the amount of methane that is actually produced could be very different from what is observed.

Finally, knowledge of the Martian dust particles is of crucial importance for the future exploration of Mars, since these particles can pose serious threats to both instrumentation and humans. Not only because these particles themselves could harm equipment, but also because in dust storms, dust particles can become electrically charged, which might result in dangerous electrical discharges (see e.g. Renno & Kok 2008, and references therein).

## 2. FLUX & POLARISATION

### 2.1 Introduction of concepts

To obtain a global overview of the Martian dust, remote sensing of the sunlight, that has been reflected by the Martian surface and scattered by the Martian atmosphere, is required. This light can be described by a vector  $\mathbf{I}$  as follows:

$$\mathbf{I} = \{I, Q, U, V, \}$$
 (1)

Where  $I$  is the total flux of the light,  $Q$  and  $U$  represent linearly polarized light and  $V$  the circularly polarized light, all with units of  $W/m^2$ . Circularly polarized flux arises typically when light is scattered by optically active or chiral particles. Recent measurements (Sparks et al. (2005)) have shown that the degree of circular polarization averaged over the face of the planet is 0.02 % (detection limit) and that no regions of circular polarization were actually identified. Because of its small value we will ignore circular polarization in the following.

The direction of the light that is incident on a planet is described by elevation angle  $\theta$  and azimuthal angle  $\varphi$ . Figure 1 shows this illumination geometry. Note that the obtainable range of azimuth and elevation angles shown in figure 1 are highly dependent on the orbit parameters of the planet-orbit platform.

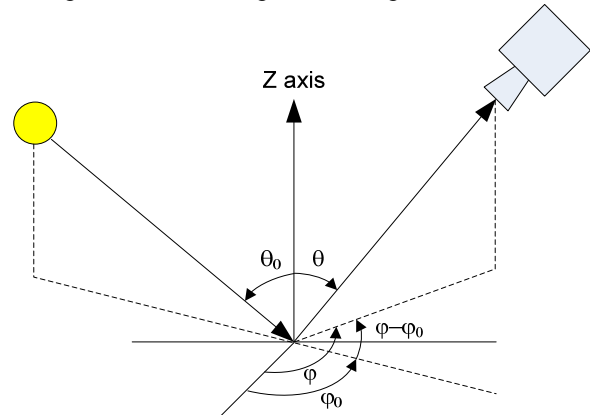


**Figure 1.** Illumination geometry of a planetary body

The degree of linear polarization  $P$  of the light is defined as shown in equation 2:

$$P = \frac{\sqrt{Q^2 + U^2}}{I}$$
 (2)

The direction of linear polarization  $\chi$ , as mathematically defined in equation 3, is defined with respect to the local meridian plane, i.e. the vertical plane containing the direction to the local nadir and the direction of propagation of the reflected light:

$$\tan(2\chi) = \frac{U}{Q}$$
 (3)

The direction of linear polarization should be in the interval  $0 \leq \chi \leq \pi$  and has the same sign as  $Q$ . Note that for  $\varphi - \varphi_0$  equal to 0 or  $\pi$  and for a horizontally homogeneous surface and atmosphere,  $\chi$  will always be equal to  $\pi/2$ .

Measuring the flux and the polarisation in combination with the scattering angle dependency proves to be a powerful tool to determine physical properties of the dust.

## 2.2 Simulated Martian radiances and degrees of linear polarization

Simulated Martian radiances and degrees of linear polarization are needed to establish requirements of and specifications for the SPEX instrument. We use the adding doubling method (de Haan et al., 1987) which contains a treatment for multiple scattering and takes into account the polarisation state of light. Figure 2 shows an example of a simulation of Martian degree of linear polarisation at 633 nm for a range of sensor geometries, where the sun elevation angle  $\theta_0$  was set to 45 degrees (see figure 1).

Main inputs for this simulation are:

- A surface albedo of 0.26. This is based on the average between maximum and minimum albedo's at this wavelength, measured by the OMEGA instrument on Mars Express (Bellucci et al., 2004).
- H<sub>2</sub>O and CO<sub>2</sub> absorption cross sections from the Hitran database (HITRAN)
- Martian Analogue Palagonite aerosol scattering expansion coefficients to represent the irregular dust particles in the Martian atmosphere (Laan et al., 2008).
- Atmospheric profiles (5 layers) for H<sub>2</sub>O concentration, CO<sub>2</sub> concentration, dust loading, temperature and pressure were derived from version 4.1 of the Mars Climate Database (MCD) (Forget et al., 2006). Inputs for the MCD are the Viking-1 landing location, a local time of 12:00 and a Solar longitude (Ls) of 270, corresponding to a dust storm maximum leading to a total OD (Optical Depth) of 4.8.

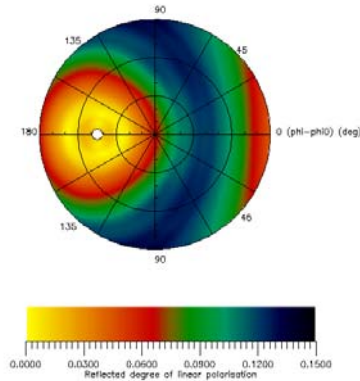


**Figure 2.** simulated reflected degree of linear polarization for a Martian dust storm scenario

It follows from this simulation that a linear degree of polarization in the range from 0.0 to 0.15 at 633 nm is foreseen for a Martian dust storm and that there is a strong angular variance.

## 3. THE SPEX INSTRUMENT

The key to understanding microphysical properties of atmospheric aerosol from remote sensing is combining flux and polarisation measurements with a range of scattering angles. In combination with the requirement to do this for a number of wavelengths and obtaining some level of coverage requires to find an instrument solution in a multidimensional space.

### 3.1 Polarisation measurement concepts

The challenge in the development of SPEX is to find an optimum solution in the choice for- and combination of spectral coverage, polarisation parameters, spatial coverage and phase angle coverage. The data product that SPEX scientists want to obtain in the end is the phase function of the atmospheric flux and polarisation (at as many different locations) as a function of wavelength.

The first challenge is to reduce the 4 dimensions of the observational space (polarisation, wavelength, coverage, phase angle) such that it can be detected with a 2-dimensional detector array. Driven by the vision to ultimately reach a compact few kg instrument we consider only options with a single telescope system, a single detector and no mechanisms, or systems that can be significantly miniaturized. The exclusion of mechanisms rules out any instrument concept such as the POLDER instrument (Leroy et al., 1997) which works with a filterwheel containing different polarisation filters and colour filters. The important advantage of the POLDER concept though, is the impressive daily global coverage capacity from low orbits due to its wide field of view, simultaneously covering an area of  $\pm 43^\circ$  along track and  $\pm 51^\circ$  cross track.

The (currently ongoing) trade-off basically boils down to 2 polarisation measurement concepts. Firstly, the conventional concept of splitting up the different polarisation states of the light directly into at least 3 separate beams, by, for example, Wollaston prisms. This method is employed in the Aerosol Polarimetry Sensor (APS) (Mishchenko et al., 2004) to be flown on NASA's Glory mission (launch currently planned for summer 2009). For a 4 beam system (APS uses 3), the degree of linear polarisation  $P$  is determined by equation 2 where follows, after doing some Mueller matrices calculus leads to equation 4 and 5:

$$\frac{Q(\lambda)}{I(\lambda)} = \frac{S_1(\lambda) - \frac{T_1(\lambda)}{T_2(\lambda)} \cdot S_2(\lambda)}{S_1(\lambda) + \frac{T_1(\lambda)}{T_2(\lambda)} \cdot S_2(\lambda)} \quad (4)$$

And

$$\frac{U(\lambda)}{I(\lambda)} = \frac{S_3(\lambda) - \frac{T_3(\lambda)}{T_4(\lambda)} \cdot S_4(\lambda)}{S_3(\lambda) + \frac{T_3(\lambda)}{T_4(\lambda)} \cdot S_4(\lambda)} \quad (5)$$

Where the intensity  $S_i(\lambda)$  is the intensity on each of the 4 beam's detectors.  $S_i(\lambda)$  is the first element of the vector  $\mathbf{S}_i(\lambda)$ , where:

$$\mathbf{S}_i(\lambda) = T_i(\lambda) \cdot M_i \cdot \mathbf{I}(\lambda) \quad (6)$$

Where  $T_i(\lambda)$  is the transmission of the optics chain from telescope to detector,  $M_i$  is the Mueller matrix for respectively a horizontal linear polarizer ( $i=1$ ), a vertical linear polarizer ( $i=2$ ), a linear polarizer at  $+45^\circ$  ( $i=3$ ) and a linear polarizer at  $-45^\circ$  ( $i=4$ ), and  $\mathbf{I}(\lambda)$  is the Stokes vector of the incoming light to the instrument.

A novel patent pending concept for measuring the polarization state was invented by Utrecht University (Snik et al., 2008) where the degree and angle of linear polarization of the incoming light is encoded as a sinusoidal modulation of the intensity spectrum. This is achieved by using an achromatic quarter-wave retarder, an athermal multiple-order retarder and a polarizing beamsplitter behind each entrance pupil.

In case there are no spectral features in the incoming light, the degree of linear polarisation  $P(\lambda)$  and the direction of linear polarization  $\chi(\lambda)$  can in principle be determined from a single measurement, as shown in equation 7:

$$S(\lambda) = T(\lambda) \cdot \frac{I(\lambda)}{2} \cdot \left( 1 \pm P(\lambda) \cdot \cos \left[ \frac{2\pi\delta(\lambda)}{\lambda} + 2\chi(\lambda) \right] \right) \quad (7)$$

Where  $S(\lambda)$  is the measured signal on the detector,  $I(\lambda)$  is the intensity spectrum and  $\delta(\lambda)$  is the retardance of the multiple-order retarder.

To be able to determine the degree and direction of linear polarisation  $P(\lambda)$  and  $\chi(\lambda)$  with a dedicated algorithm to Eq. 7, it is required that the retardance is

chosen such that the modulation is much longer than the wavelength resolution of the spectrometer.

Table 3.1 shows a high level trade-off assessment between the conventional and the modulation concept for polarisation measurement, as described in the former.

	Conventional	Modulation
<b>Number of beams</b>	At least 3, typically 4	1, preferably 2
<b>Spectrograph resolution</b>	Relates directly to scientific data product resolution	Should be much smaller than the chosen modulation period
<b>Polarization sensitivity to noise and variations between beam optics</b>	High (parameters are obtained through addition and subtraction of independent measurements)	Low (parameters are obtained twice through curve fitting of one measurement)
<b>Signal level at detector</b>	High (spectral sampling relates directly to scientific data product resolution)	Low (spectral sampling relates to the chosen modulation and is in general smaller than the spectral sampling of the conventional method)
<b>Dispersion</b>	Prism	Grating
<b>Wavelength range</b>	Determined by scientific data product	Limited by grating choice and $\lambda_{\min} < \lambda < 2 \cdot \lambda_{\min}$

**Table 3.1.** High level trade-off between the conventional and the modulation concept for polarisation measurement.

The trade-off between the conventional and the modulation concept is ongoing. We foresee to use a Cramér–Rao lower bound (CRLB) analysis to make a proper comparison between the two. It has already been shown by Snik et al. (2008), that the modulation method is able to comply to the science requirements for polarization sensitivity and accuracy (see table 3.2). As such, the current SPEX instrument baseline is the modulation concept for which we will create a breadboard to show system level feasibility.

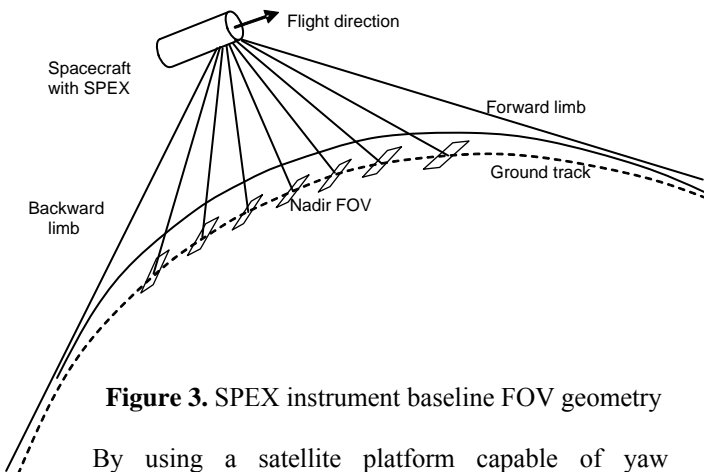
### 3.2 SPEX instrument baseline specification

Table 3.2 shows the baseline specification / requirement of the SPEX instrument. This set of parameters is derived in an iteration between science and engineering.

Parameter	Value
Spectral range	400-800 nm
Spectral resolution	2 nm
Spectral sampling	1 nm
Aperture diameter	1 mm
Data-product spectral sampling	20 nm
Viewing directions	9 in total: 0°, +/- 18°, +/- 36°, +/- 54° limb forward, limb backward
FOV per viewing direction	8° (across track, swath width) x 1.7° (along track)
Polarization sensitivity	0.5 % degree of linear polarization
Polarization accuracy	5 % (minimum)
Mass of SPEX spectropolarimeter, subsystem	2 kg (target)
Dim. of SPEX spectropolarimeter subsystem	130 x 130 x 60 mm <sup>3</sup>
Power requirement	Operation of CMOS detector: < 0.5 W No mechanisms in the instrument
Temperature requirement	Close to room temperature
Operational constraints	Measurements are only required at the sunlit side of the planet of interest. Pointing knowledge and stability of platform should be better than 360 arcsec.
Data rate requirement	0.5 Gbit/day (Mars to Earth data rate)

**Table 3.2.** SPEX instrument baseline requirements and specifications

The SPEX instrument baseline has 7 nadir looking FOV's which allow phase angle coverage by overflight of the area of interest. Additional forward and backward limb FOV's are present to extend the phase angle range for a given area of interest as much as possible. Figure 3 shows the geometry of the SPEX instrument baseline FOV's.



**Figure 3.** SPEX instrument baseline FOV geometry

By using a satellite platform capable of yaw oscillation steering, it proves to be possible to obtain scientific data for all the points in the 7° swath width of the nadir pointed telescope. Without this

capability, only part of the scientific data within the 7° swath width is available for the fully achievable scattering range. This is caused by the fact that during overflight of the area of interest, this area rotates away from the orbit plane.

Figure 4 shows a CAD drawing of the optical design of SPEX.

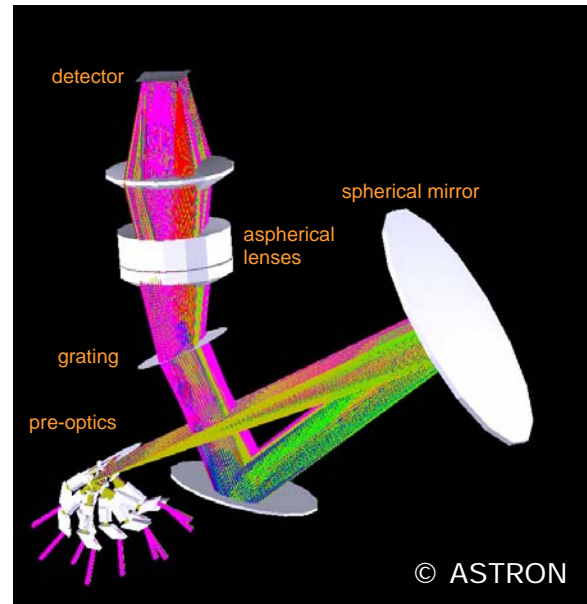


**Figure 4.** SPEX instrument baseline optical design

The Martian radiance enters the pre-optics which contains 9 telescope systems which include the polarization modulation optics. Each telescope system contains 2 output beams each having an opposite modulation in its spectrum (see '±' sign in Eq. 7). The advantage of having these 2 opposite modulation spectra is that an un-modulated high resolution spectrum can be obtained by combining them. This spectrum is also foreseen to play an important role in further improving the accuracy of the polarization data products that could already be obtained by any of the 2 modulated spectra.

The 18 output beams from the pre-optics are combined in to a single plane to go through the spectrometer slit. From there on, this plane is imaged onto a 2D detector after dispersion by a transmission grating. The detector we foresee to use is the (space qualified) Cypress Star 250 CMOS detector, with associated control electronics, 512 x 512, 25 μm pitch pixels, reasonable quantum efficiency from 400 to 800 nm and built in 10-bits ADC.

Figure 5 shows a simulated signal for one detector row (i.e. one of the spectra measured within a single SPEX FOV), with an integration time of 3 seconds. The inputs for the radiative transfer model to obtain this simulated signal are as presented in section 2.2. The elevation angle  $\theta$  for the sensor was set to 0 degrees (i.e. strictly nadir).

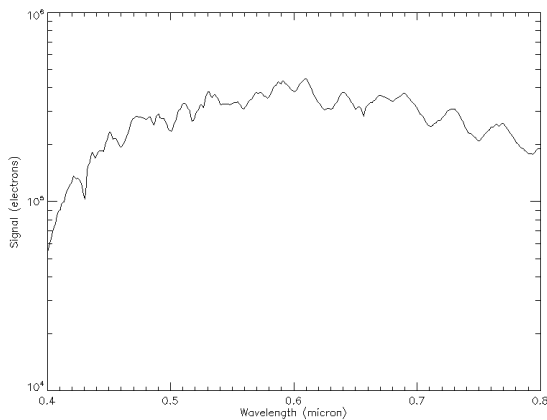


**Figure 5.** Simulated SPEX signal as a function of wavelength

The features in the signal are a combination of Fraunhofer lines present in the solar irradiance and the modulation introduced by the telescope modulator optics. The latter features are best seen between 700 and 800 nm where the features of the solar irradiance Fraunhofer lines are slightly less pronounced. From the amplitude of the observed modulation, the degree of linear polarisation could be determined and should be in the order of 6 % (with reference to figure 2).

## REFERENCES

Mishchenko, M.I., B. Cairns, J.E. Hansen, L.D. Travis, R. Burg, Y.J. Kaufman, J.V. Martins, and E.P. Shettle 2004. Monitoring of aerosol forcing of climate from space: analysis of measurement requirements. *J. Quant. Spectrosc. Radiat. Transfer* 88, 149-161.

F. Snik, Th. Karalidi, Ch. Keller, E. Laan, R. Ter Horst, R. Navarro, D.M. Stam, Ch. Aas, J. de Vries, G. Oomen, R. Hoozeveld. SPEX: An in-orbit spectropolarimeter for planetary exploration. In *SPIE Astronomical Instrumentation*, 23-28 June, Marseille, France, 2008.2008, *Proc. SPIE*, Vol. 7010, 701015 (2008); DOI:10.1117/12.787218

Leroy M., Deuze J.L., Bréon F.M., Hauteceur O., Herman M., Buriez J.C., Tanre D., Bouffies S., Chazette P., and Roujean J.L., 1997 :

Retrieval of atmospheric properties and surface bidirectional reflectances over the land from POLDER.

*Journal of Geophysical Research.*, vol 102, #D14, pp17023-17037, July 27th 1997

de Haan J.F, Bosma P.B., Hovenier J.W., The adding method for multiple scattering calculations of polarized light, *Astron. Astrophys*, 183, 371-391 (1987)

Bellucci, G, Altieri, F, Bibring, J.-P. and the OMEGA Team, The OMEGA Instrument on board Mars Express: First Results, *Memorie della Societa Astronomica Italiana Supplement*, 2004, volume 5

Forget, F., Millour, E., Lebonnois, S., Montabone, L., Dassas, K., Lewis, S. R., Read, P. L., López-Valverde, M. A., González-Galindo, F.; Montmessin, F.; Lefèvre, F.; Desjean, M.-C.; Huot, J.-P., The new Mars climate database, *Mars Atmosphere Modelling and Observations* (book), 2006

HITRAN-High-resolution TRANsmission molecular absorption database (<http://cfa-www.harvard.edu/hitran>)

Laan E.C, Volten H, Stam D.M., Muñoz O, Hovenier J.W., Roush T.L., Scattering matrices and expansion coefficients of Martian analogue palagonite particles, accepted for publication in *Icarus* (August 2008)

Pearl, J. C., Smith, M. D., Conrath, B. J., Bandfield, J. L., & Christensen, P. R. 2001, *J. Geophys. Res.*, 106, 12325

Gierasch, P. J. & Goody, R. M. 1972, *Journal of Atmospheric Sciences*, 29, 400

Goldenson, N., Desch, S., & Christensen, P. 2008, *Geophys. Res. Lett.*, 35, 8813

Montmessin, F., Forget, F., Rannou, P., Cabane, M., & Haberle, R. M. 2004, *Journal of Geophysical Research* (Planets), 109, 10004

Määttänen, A., Vehkamäki, H., Lauri, A., et al. 2005, *Journal of Geophysical Research* (Planets), 110, 2002

Atreya, S.K., Mahaffy, P.R., & Wong, A.-S. 2007, *Planet. Sci.*, 55, 358

Renno, N.O. & Kok, J.F., 2008, *Space Science Reviews*

W. B. Sparks, J. H. Hough, and L. E. Bergeron. A Search for Chiral Signatures on Mars. *Astrobiology*, 5:737-748, 2005. doi: 10.1089/ast.2005.5.737.